Time-reversible Molecular Motion and Macroscopic Irreversibility

Harald A. Posch

Institut für Experimentalphysik, Universität Wien, Boltzmanngasse 5, A-1090 Wien, Austria

William G. Hoover*

Department of Physics, Keio University, Yokohama 223, Japan

Brad Lee Holian

Theoretical Division, Los Alamos National Laboratory, Los Alamos, New Mexico 87545, USA

Computer Experiments / Nonequilibrium Phenomena / Nonlinear Phenomena / Statistical Mechanics / Transport Properties

The thermodynamic irreversibility of molecular processes involving heat transfer is established by incorporating time-reversible dynamical thermostats in the equations of motion. It is then possible to understand why nonequilibrium steady states *must* obey the Second Law of Thermodynamics, not just with high probability, but *with probability one*. This is because nonequilibrium states are *so rare*, relative to equilibrium ones, as to occupy a zero-volume multifractal part of equilibrium phase space. These conclusions are generally valid. We illustrate them here by studying equilibrium manybody systems, both solid and fluid, as well as a simple one-body chaotic nonequilibrium steady state. In all these cases we follow the motion of an orthonormal set of comoving vectors $\{\delta\}$, determining the time-averaged "Lyapunov Spectrum" of dynamic instability rates, as well as the vectors "Rotation Spectrum", and relating these spectra to the irreversible nature of nonequilibrium flows described above.

1. Introduction

The dynamical properties of fluids and solids have been extensively studied both experimentally and by computer simulation [1]. For systems in thermodynamic equilibrium the main emphasis has been on the determination of time correlation functions of dynamical variables, for nonequilibrium systems on the evaluation of the in general non-linear response of the system due to an applied perturbation $X(t)$. Only in the limit of vanishing X it is possible to relate the transport coefficients to time integrals of equilibrium correlation functions of their respective currents. These are the famous Green-Kubo integrals [2–4] forming the basis of many simulation studies of transport phenomena. For finite X, however, the phase-space distribution function $f(\Gamma, t)$ is not a well behaved and smooth function of the phase variables Γ. For this particular reason the non-linear response theory is not in an advanced stage, the consequences of the singular nature of $f(\Gamma, t)$ having been discussed [5] only recently.

In this paper we review the evidence we have from nonequilibrium molecular dynamics simulations, which may help to understand irreversible behaviour of systems in nonequilibrium steady states. The key to this problem is the evaluation of the sensitivity of a trajectory in phase space to small, actually infinitesimal, perturbations of its initial conditions. This property may be expressed in terms of Lyapunov characteristic exponents, the whole set being referred to as the "Lyapunov spectrum" of the system. The Lyapunov exponents describe the exponential spreading apart of neighbouring phase-space trajectories and will be discussed in more detail in Section 3. In the course of time the separation vectors $\delta(t)$ between such neighbouring trajectories not only change their norms but also their orientations in phase space. This serves to define characteristic rotation numbers [6], the whole set being referred to as the "rotation spectrum". In Section 4 we present new results for the Lyapunov- and rotation spectra of an equilibrium 32-particle system in three dimensions. Both liquid and solid states are considered. These are probably the first calculations of rotation spectra for many-particle systems.

The sensitivity of the equations of motion to small variations of the initial conditions is responsible for the irreversible approach to equilibrium in accordance with the Second Law of thermodynamics. From simulations of the Lyapunov spectra of nonequilibrium systems in steady states one finds that the nonequilibrium distribution function $f(\Gamma, t)$ collapses onto a fractal attracting subset of zero phase-space volume. This is demonstrated in Section 5 for a simple one-dimensional conductivity model. It is shown for this particular example that the underlying strange attractor is a "multifractal" set with a whole spectrum of dimensions D_q. The information dimension D_1 is significantly smaller than the Hausdorff (capacity) dimension, which in turn is smaller than the dimension $D = 3$ of the phase space. This indicates that this system is not ergodic. In another example of comparable complexity studied by Hoover and Moran [7] – nonequilibrium diffusive flow, periodic in space but stationary in time [8,9] – the Hausdorff dimension agrees with D; this system seems to be ergodic and mixing, even far from equilibrium.

The appearance of fractal attractors of zero phase-space volume provides the basis for a geometrical interpretation of the irreversible behaviour found in such nonequilibrium steady-state systems. The arrow in time exists in spite of the time-reversal invariance of the underlying phase-space dynamics. This connention with the Second Law will be dis-

*) Permanent address: Department of Applied Science, University of California at Davis-Livermore and Lawrence Livermore National Laboratory, Livermore, California 94550, USA.

cussed in Section 6. The essential step to bridge this gap is the use of recently developed time-reversible equations of motion interacting with macroscopic heat reservoirs. The essence of this method will be shortly described in the following Section.

2. Nonequilibrium Molecular Dynamics and Heat Baths

In a nonequilibrium system any external perturbation $X(t)$ will perform work on the system. As this work is dissipated into heat a continuous increase of temperature results. To achieve nonequilibrium steady state conditions a deterministic feedback mechanism has to be introduced, which according to Nosé [10, 11] and Hoover [12] shows up in the equations of motion as an additional constraining force term. As an example we consider in the following mass conductivity of N particles in an external field $X(t)$ – such as an electric field acting on charged particles carrying unit charges $c = \pm 1$. The equations of motion are [14]:

$$\dot{\Gamma} = \begin{cases} \dot{q} = p/m \\ \dot{p} = F(q) + cX(t) - \zeta \tilde{p} \\ \dot{\zeta} = (K/K_0 - 1)/\tau^2 . \end{cases} \tag{1}$$

Here, $\Gamma = (q, p, \zeta)$ denotes a point in phase space, where q stands for all coordinates, and p for the momenta. $\tilde{p} = p - \sum^{c} p/N_c$ is the peculiar momentum of a particle relative to the center of mass of the N_c particles carrying a charge c (over which the sum $\sum^{c}$ has to be performed. ζ is a single additional variable representing the action of the thermostat. $K = \sum \tilde{p}^2/2m$ is the instantaneous peculiar kinetic energy, and $K_0 = gkT/2$ its long-time averaged value. The sum is over all particles, and g denotes the momentum degrees of freedom. k_B is Boltzmann's constant. $F = -\partial \Phi/\partial q$ is the intrinsic force with $\Phi(q)$ the potential energy. In (1) the equation for each particle is modified by the feedback term $-\zeta \tilde{p}$ and the thermostat is homogeneous. If only boundary particles are affected, the method is inhomogeneous. In any case, some form of thermostatting is essential for achieving nonequilibrium steady states.

The parameter τ in (1) is the response time of the thermostat and is usually chosen to be of the order of a collision time. In the limit $\tau \to \infty$ Newton's equations of motion are recovered. In the opposite limit of infinitely fast response the equations are equivalent to evolution equations derived from Gauss' principle of least constraint which keeps the kinetic energy exactly constant (isokinetic simulation) [15, 16].

Under equilibrium conditions ($X(t) = 0$) the Nosé-Hoover Eqs. (1) generate a canonical ensemble, provided that the system is ergodic and mixing. The equilibrium phase-space distributions assumes the canonical form

$$f_0(\Gamma) = \frac{1}{Z} \exp[-\beta H_0(q,p) - (1/2) g \tau^2 \zeta^2] , \tag{2}$$

where $H_0 = K + \Phi$ is the internal energy, $\beta = 1/k_B T$, and the partition function $Z = \int d\Gamma \exp[-\beta H_0 - (1/2) g \tau^2 \zeta^2]$. The dimension of phase space for Nosé-Hoover mechanics is $2dN + 1$, d being the dimension of space and N the number of particles. The extra dimension is contributed by the thermostat variable ζ.

To achieve a nonequilibrium steady state the external field $X(t)$ is switched on at $t = 0$ and is held constant afterwards, $X(t > 0) = X$. After the decay of initial transients the steady-state average of the dissipative flux $J = \Sigma c p/m$ serves to define a conductivity σ which in general still depends on the magnitude of the external field:

$$\langle J \rangle = \sigma(X) X . \tag{3}$$

The rate of work performed *on* the system by the field is given by $\dot{W} = \langle J \rangle \cdot X$. For steady states this is equal to the rate at which the generated heat is removed *from* the system by the thermostat. This energy balance establishes that

$$\langle \zeta \rangle = \frac{\langle J \rangle \cdot X}{2K_0} = \frac{1}{g} \langle \Lambda \rangle , \tag{4}$$

where, as before, g denotes the thermostatted momentum degrees of freedom. The last equality relates the thermostat variable to the rate of logarithmic phase-space expansion, $\Lambda \equiv (\partial/\partial \Gamma \cdot \dot{\Gamma}(\Gamma, t)$. This important relation will be used below.

We want to stress that the Nosé-Hoover equations of motion or the related equations based on Gauss' isokinetic mechanics are time reversible. This means that replacing t by $-t$ and all momentum-like variables p, ζ by $-p, -\zeta$ leaves the equations of motion unchanged. Nevertheless, under nonequilibrium steady-state conditions they always give positive friction coefficients $\langle \zeta \rangle$ in accordance with the Second Law. We shall come back to this point in the following sections.

The particular example (1) is for mass flow in an external field. Equivalent formulations of Nosé-Hoover or Gauss equations of motion for other transport phenomena such as shear viscosity or heat conductivity have been discussed by Evans, Hoover and others [15–19].

3. Lyapunov and Rotation Spectra

The fundamental property of a chaotic system is the sensitivity of its phase-space trajectory to a small perturbation of the initial conditions. If the flow Eqs. (1) are abbreviated as

$$\dot{\Gamma}(t) = G(\Gamma(t)) , \tag{5}$$

an infinitesimal perturbation $(\delta \Gamma)_l \equiv \delta_l$ develops in time according to the linearized equations

$$\dot{\delta}_l = D(\Gamma(t)) \cdot \delta_l(t) , \tag{6}$$

where the dynamical $D \times D$ matrix $D(\Gamma) = \partial G/\partial \Gamma$ couples the reference trajectory $\Gamma(t)$ to the time evolution in tangent space of the differential offset vectors $\delta_l(t)$. In a D-dimensional phase space there are D linearly independent vectors δ_l, $l = 1, \ldots, D$. Their formal solution may be written as

$$\delta_l(t) = \boldsymbol{L}(t;0)\,\delta_l(0)\,, \tag{7}$$

where the propagator $\boldsymbol{L}$ is a time-ordered exponential [21]:

$$\boldsymbol{L}(t;0) = \exp_+\left\{\int_0^t \boldsymbol{D}(\boldsymbol{\Gamma}(t'))\,\mathrm{d}t'\right\}. \tag{8}$$

Oseledec showed [20] that for sufficiently well-behaved flow equations such as (1) there exists for almost every $\boldsymbol{\Gamma}(0)$ a set of orthonormal vectors $\delta_l(0)$ with lengths diverging or converging exponentially with time. The corresponding rate constants

$$\lambda_l = \lim_{t\to\infty}\frac{1}{t}\ln|\boldsymbol{L}(t;0)\,\delta_l(0)| \tag{9}$$

are independent of $\boldsymbol{\Gamma}(0)$ and are called the Lyapunov characteristic exponents. The whole set $\{\lambda_l\}$ is referred to as the Lyapunov spectrum of the system. For convenience the λ_l are ordered from largest to smallest, $\lambda_1 \geq \lambda_2 \geq \ldots \geq \lambda_D$.

From a practical point of view the precise orientation of all initial vectors $\{\delta_l(0)\}$ is not known nor is it needed for the determination of the Lyapunov spectrum. Any arbitrarily oriented set of orthonormal vectors will do. However, these vectors will not stay orthonormal for $t > 0$ but will start rotating into the direction of largest phase-space growth and eventually diverge. In the classical algorithms developed by Benettin and others [22–24] this is prevented by reorthonormalizing the vectors periodically after a certain number of time steps. In a more refined and continuous algorithm the vectors $\delta_l(t)$ are constrained to remain orthonormal for $t > 0$, and the Lyapunov exponents are calculated from the time-averaged Lagrange multipliers contained in the constraining forces [14, 21, 25, 26]. λ_1 gives the time-averaged rate at which pairs of neighboring phase trajectories diverge or converge exponentially, $\lambda_1 + \lambda_2$ the rate of divergence or convergence of a small comoving phase-space area, and finally $\lambda_1 + \ldots + \lambda_l$ the rate of divergence or convergence of a small l-dimensional phase-space object. For a chaotic system at least one of the exponents, λ_i, has to be positive.

If the time average in (9) is explicitly written as

$$\lambda_l = \lim_{t\to\infty}\frac{1}{t}\int_0^t \lambda_l(t')\,\mathrm{d}t'\,, \tag{10}$$

the time dependent integrand $\lambda_l(t)$ is given by

$$\lambda_l(t) = \frac{\mathrm{d}}{\mathrm{d}t}\ln|\delta_l(t)|\,. \tag{11}$$

It may fluctuate considerably around its mean. In the case of a chaotic flexible pendulum the root-mean-square fluctuation of $\lambda_l(t)$ may exceed λ_l by a factor of 10 [27]. The fluctuations around the mean depend on the choice of coordinates and can be made arbitrarily large.

In addition to the stretching or contraction of the vectors $\delta_l(t)$ for $t > 0$ they are also constantly reoriented with an instantaneous angular frequency $\omega_l(t)$. The propagator (8) may be written as $\boldsymbol{L} = \boldsymbol{RS}$, where $\boldsymbol{S}$ performs the expansion or contraction operation, and $\boldsymbol{R}$ is a unitary rotation [21]. The time averages

$$\omega_l = \lim_{t\to\infty}\frac{1}{t}\int_0^t \omega_l(t')\,\mathrm{d}t' \tag{12}$$

define "rotation numbers" ω_l. Their whole set will be referred to as the "rotation spectrum" [6].

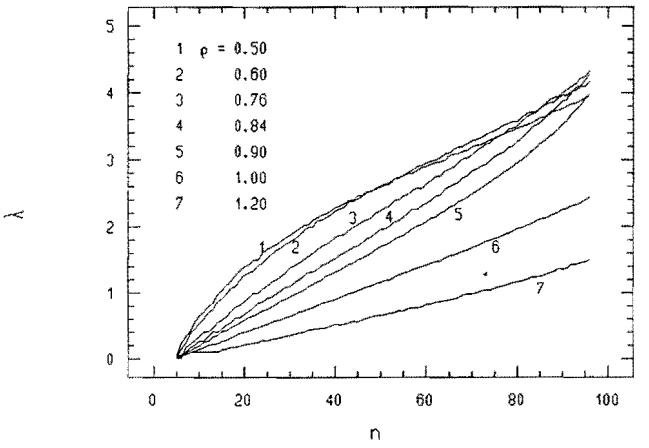

Fig. 1
Lyapunov spectra for various equilibrium states on the isotherm $k_B T/\varepsilon = 1.15$. The densities are indicated by the labels. Although the exponents are defined only for integer values of the index n, they are connected by a smooth line to enhance clarity. Only the positive branches of the spectra are shown such that $\lambda_{\max}$ is associated with $n = 96$ and the smallest positive exponent with $n = 5$. All quantities are given in reduced units

4. Simulation of Equilibrium Systems

In this section we report Lyapunov spectra for equilibrium systems consisting of $N = 32$ particles in three dimensions over the whole range of liquid and solid densities. Though no thermostat is needed for such a simulation, we use an isokinetic Gaussian thermostat in the equations of motion which defines the desired temperature for a given density. A Nosé-Hoover thermostat as in (1) – with vanishing external perturbation $X(t)$ and generating a canonical ensemble – would serve the same purpose, the Lyapunov spectra being insensitive to the ensemble used for the simulation [14, 28]. Equilibrium systems evolving according to time-reversible equations of motion have symmetric Lyapunov spectra: for each positive exponent there is a negative one with equal absolute magnitude. Therefore only the positive branches of the spectra are shown in Fig. 1. There are seven constants of the motion – center of mass, momentum and kinetic energy. Since the exponents always appear in pairs of opposite sign, eight exponents out of a total of 192 must vanish. This is confirmed by the simulation. The vanishing exponents are not included in Fig. 1.

For the calculation of the Lyapunov spectra the usual periodic boundary conditions must be implemented with care. To strictly conserve the center of mass the periodic boundaries must be used only for the calculation of the forces. In our simulation the particles interact with a Len-

nard-Jones potential which is smoothly truncated at $r/\sigma = \sqrt{3}$ by fitting a cubic spline at the inflection point $(26/7)^{1/6}\sigma$ [29, 30]. Lennard-Jones reduced units are used throughout, for which the well depth ε, the range σ, and the particle mass m are unity. The unit of time is therefore $\tau = \sigma(m/\varepsilon)^{1/2}$. For the simulation of L exponents $2dN(L+1)$ differential equations of first order have to be integrated simultaneously. In our case $(L = D/2)$ this requires the simultaneous solution of more than 18000 equations for at least 300 time units. A fourth-order Runge-Kutta integrator with a time step 0.001 was used.

All spectra in Fig. 1 correspond to the constant temperature $k_B T/\varepsilon = 1.15$. The densities ϱ vary from 0.5 to 1.2. The shape of the spectrum changes qualitatively from the liquid to the solid [28] and can be roughly described by power laws reminiscent of Debye's crystal-frequency distributions: $\lambda(n) = \alpha[n - (c/2)]^{\beta}$. n is an index associated with an exponent such that $n = D/2 = 96$ for the largest, and $n = 5$ for the smallest positive exponent. $c = 8$ is the number of vanishing exponents. For the liquid states β is of the order of 1/3 [14] and becomes larger than one for the solid [28]. Analogous results have also been obtained for systems in two [28] and one [31] dimensions.

In Fig. 2 the largest Lyapunov exponent is plotted for states on the 1.15-isotherm as a function of density. For ϱ near the liquid-solid phase transition it reaches a maximum which indicates very fast dynamical events and efficient mixing in the system.

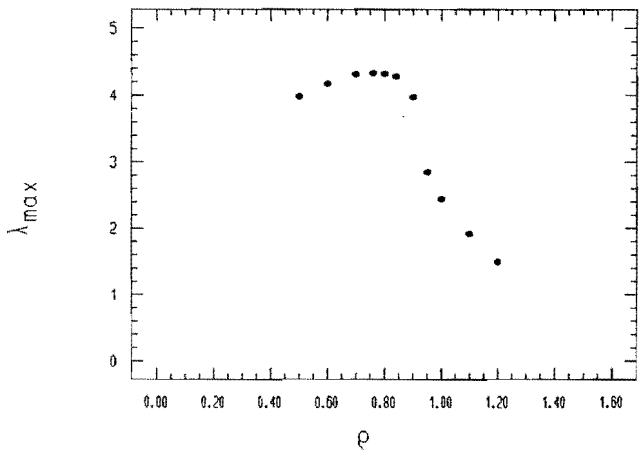

Fig. 2
Variation of the largest Lyapunov exponent λ_{max} as a function of the density ϱ for equilibrium states on the isotherm $k_B T/\varepsilon = 1.15$

The rotation spectra for some of the states on the same isotherm are plotted in Fig. 3 as a function of the index n introduced above. For the same reasons as for the Lyapunov spectra the rotation spectra are also symmetric: there are always two identical positive rotation numbers associated with the two Lyapunov exponents equal in absolute magnitude. Therefore only one branch of the various rotation spectra is shown. For larger indices $n \gtrsim 10$ the spectra are smooth and well behaved. For small n, however, for which the Lyapunov exponents are very small or identical to zero, the rotation spectra show a very pronounced fine structure. The origin of this feature is not clear. The spectra vary smoothly with density and show no anomaly near the liquid solid phase transition. It is interesting to note that the offset vectors $\delta_l(t)$ pointing into phase-space directions expanding or contracting violently rotate rather slowly, whereas phase-space directions associated with vanishing Lyapunov exponents cause these vectors to reorient with fast angular velocity.

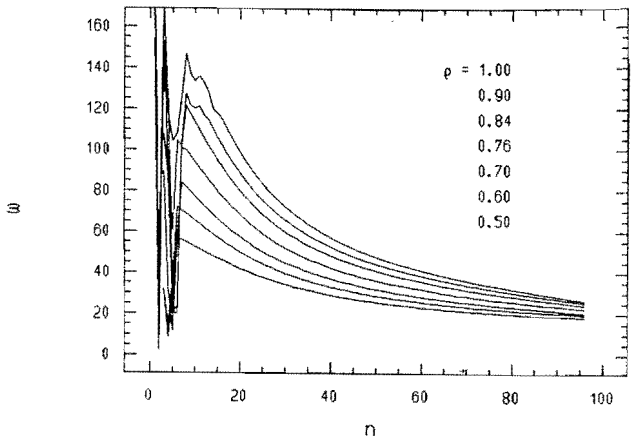

Fig. 3
Rotation spectra for various equilibrium states on the isotherm $k_B T/\varepsilon = 1.15$. The density decreases from the top to the bottom curve as indicated in the figure. No anomaly due to the solid-liquid phase transition is observed. The rotation indices are defined only for integer n. The 96 rotation numbers shown for each spectrum are smoothly connected to enhance the clarity of the figure and correspond to the positive branch of the respective Lyapunov spectrum. The remaining 96 numbers for each spectrum not shown in the figure are symmetrical around $n = 0$. Lennard-Jones reduced units are used as defined in Section 4

5. Systems in Nonequilibrium Steady States

If the external field in (1) is switched on at $t = 0$ and held constant, $X(t) = X\Theta(t)$, the system approaches a steady state after the decay of some transient behaviour [5]. To see what the consequences for the phase trajectory are it is advantageous to study a simple low-dimensional example such as the one-dimensional conductivity of a single particle in a periodic potential and subjected to an external field [32]. The equations of motion (1) simplify considerably and may be written in appropriate reduced units as

$$\begin{aligned} \dot{x} &= p \\ \dot{p} &= -\sin x + X - \zeta p \\ \dot{\zeta} &= (p^2 - 1)/\tau^2 . \end{aligned} \tag{13}$$

The phase space is periodic in x-direction with periodicity 2π. The simulation reveals chaotic trajectories [32] for certain values of the parameters X and τ. In Fig. 4 the Poincaré map for $x = 2\pi i$, i integer, is shown for $1/\tau^2 = 0.1$ and $F = 0.3$. Clearly, the phase space visited by the trajectory is a strange attractor. Its Lyapunov dimension may be deduced from the Lyapunov exponents $\lambda = \{0.0393, 0, -0.0842\}$ with the help of the Kaplan-Yorke formula [33, 34]. One finds $D_L = 2.47$, which is significantly smaller than three, the phase-space dimension for this case.

This finding can be strengthened by evaluating the whole multifractal spectrum of singularities $f(\alpha)$, where α is the strength of the singularity [35, 36]. The singularity spectrum is related to the generalized Renyi dimensions D_q defined as

$$D_q = \frac{1}{q-1} \lim_{L \to 0} \frac{\ln \sum_i p_i^q(L)}{\ln L} . \tag{14}$$

If the whole attractor is covered with boxes of size L, $p_i(L)$ in (14) denotes the probability of the trajectory to be in box i (measure integrated over i). q is a "microscope parameter" which emphasizes regions in phase space according to their singularity strength: $q > 1$ gives more weight to regions characterized by large α, and $q < 1$ accentuates regions with weak singularities. If $f(\alpha)$ is known the Renyi dimensions can be obtained from

$$D_q = \frac{1}{q-1} [q\alpha(q) - f(\alpha(q))] . \tag{15}$$

D_0 is the Haudorff dimension, which is the dimension of the support of the measure, D_1 is the information dimension, and D_2 is the correlation dimension introduced by Grassberger and Procaccia [36, 37].

The method of Chhabra and Jensen [38] was used for the evaluation of $\alpha(q)$ and $f(\alpha(q))$ according to

$$\alpha(q) = \lim_{L \to \infty} \frac{\sum_i \mu_i(q, L) \ln [p_i(L)]}{\ln L} \tag{16}$$

$$f(q) = \lim_{L \to \infty} \frac{\sum_i \mu_i(q, L) \ln [\mu_i(q, L)]}{\ln L} \tag{17}$$

where

$$\mu_i(q, L) = p_i^q(l) / \sum_j p_j^q(L) \tag{18}$$

is also a normalized invariant measure. If the respective numerators of (16) and (17) are plotted against $\ln L$ for various L, α and f may be determined from the limiting slopes. Since this method is a box counting algorithm which requires a significant amount of storage on a computer, it was not applied to the total attractor but to the Poincaré section of Fig. 4. The dimension of the total attractor is obtained by adding unity to the section dimensions. The whole Poincaré map was covered with 1024×1024 boxes and three million points of the map were used to define $p_i(L)$. The result is depicted in Fig. 5 with the parameter q indicated by the labels.

The information dimension $D_1 = f(\alpha(1)) = 2.47$ agrees very well with the Lyapunov dimension found above and is a very useful parameter for characterizing the attractor. The method, however, did not converge well for $q = 0$. Therefore the Hausdorff dimension was obtained only by extrapolation (smooth line) from the maximum of $f(\alpha)$. In spite of this ambiguity D_0 is significantly lower than three, the phase space dimension. This indicates that for this particular one-dimensional conductivity model even the support of the measure for the attractor has a vanishing volume in phase

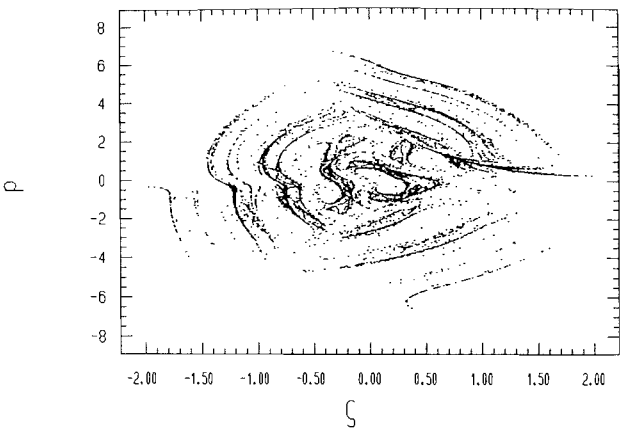

Fig. 4
Poincaré map of sections defined by $x = 2\pi j$, j integer, for the one-dimensional conductivity model discussed in Section 5. 10000 points are shown

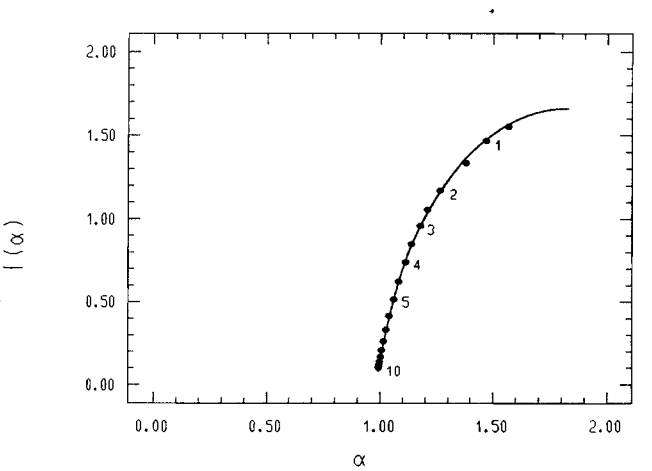

Fig. 5
Multifractal spectrum of singularities $f(\alpha)$ as a function of the singularity strength α for the Poincaré section of Fig. 4. The value of the parameter q is indicated by the label. The smooth curve is an extrapolation to $q = 0$. To obtain the Renyi dimensions D_q for the one-dimensional conductivity model discussed in Section 5, unity has to be added to $f(\alpha(q))$

space. In a similar study of a two-body Lorentz gas the Hausdorff dimension was found to agree with the phase-space dimension, but the information dimension was significantly smaller [7]. We believe that this is the generic case for many-body systems in two or three dimensions.

The main conclusion of this section is that for nonequilibrium systems in steady states the information dimension D_1 is smaller than the phase-space dimension D. This follows directly from the Nosé-Hoover equations of motion and the geometric requirement that the occupied volume cannot diverge. The sum over all Lyapunov coefficients may be related to the logarithmic rate of phase-space expansion introduced in section 2,

$$\langle \Lambda \rangle = -g \langle \zeta \rangle = \sum \lambda , \tag{19}$$

and is always negative. This means that the full Lyapunov spectrum is not symmetric any more and is shifted to more

negative values. The details of its shape depend also on the boundary conditions whether a homogeneous or heterogeneous thermostat is used [14, 28]. These general results have been verified in a variety of nonequilibrium systems such as a periodic two-dimensional Lorentz gas driven by an external field [7–9], isokinetic two-body planar shear flow [39–42], conductivity in a 32-body system governed by the equations of motion (1) [14], and manybody boundary-driven shear flow in two and three dimensions [28].

6. Strange Attractors and Irreversibility

In the previous section it was shown that the nonequilibrium distribution function $f(\Gamma, t)$ for systems in nonequilibrium steady states collapses onto a strange attractor which is a fractal subset of the phase space with information dimension D_1 smaller than the phase-space dimension D. Therefore its phase-space volume is not just small but vanishes exactly. The collapse manifests itself in a negative sum over all Lyapunov exponents which according to (19) means that the time-averaged "friction" variable $\langle\zeta\rangle$ is always positive in accordance with the Second Law. According to (4) this is also the case for W, the rate of work performed on the system by the external perturbation X. Along an infinitely long trajectory work is always converted into heat, never the reverse. The only trajectory capable of converting heat into work and consequently violating the Second Law would have to be located precisely on the "strange repellor". These repellor states could in theory be obtained by applying the time-reversal transformation $(q \to q, p \to -p, \zeta \to -\zeta$ to all states on the attractor. By construction the repellor is again a strange fractal set with vanishing phase-space volume. Because of this, the probability of locating a reversed trajectory on the repellor is zero, not just small. Furthermore, time reversal also changes all signs of the Lyapunov exponents and the repellor states are characterized by a positive sum of all exponents and are inherently unstable. Any slightest deviation of the reversed trajectory from the repellor immediately blows up exponentially and the system trajectory approaches the attractor again.

The situation can be summarized as follows [32, 43]: Because of the vanishing phase-space volume of the attractor the time-reversed trajectory cannot be localized *exactly* on the repellor, and because of the instability of the repellor states any attempt of localizing it *approximately* on the repellor is doomed to fail after a time of the order of $1/h_K$, where h_K is the Kolmogorov entropy given by the sum of all *positive* Lyapunov exponents of the system. The geometrical concept of fractal strange attractors and repellors in the phase space of nonequilibrium steady-state systems resolves the famous reversibility paradox formulated by Loschmidt in 1876 [44]. To counter these objections Boltzmann introduced statistical arguments arguing that equilibrium states by far outnumber nonequilibrium states and cause closed systems with overwhelming probability to approach equilibrium [45]. In our geometrical interpretation [43], which makes use of a *time-reversible* thermostat coupled to the system, the probability of violating the Second Law is not just small, it actually vanishes.

The computations were performed at the computing center of the University of Vienna within the framework of IBM's European Supercomputing Initiative. We gratefully acknowledge the generous allocation of computer time. We also thank Dr. John Hague, IBM-UK, for his assistance with the vectorization of some of the programs, Mag. Aharon Majerowicz for his help with the computer graphics, and Dr. S. Ruffo for bringing Ref. [6] to our attention.

References

[1] Articles, in: Molecular-Dynamics Simulation of Statistical-Mechanical Systems, Course XCVII of Proc. Int. School of Physics Enrico Fermi, Varenna, eds. G. Ciccotti and W. G. Hoover, North-Holland, Amsterdam 1986.
[2] M. S. Green, J. Chem. Phys. *20*, 1281 (1952); *22*, 398 (1954).
[3] R. Kubo, J. Phys. Soc. (Jpn.) *12*, 570 (1957).
[4] R. Zwanzig, Ann. Rev. Phys. Chem. *16*, 67 (1965).
[5] B. L. Holian, G. Ciccotti, W. G. Hoover, B. Moran, and H. A. Posch, Phys. Rev. A *39*, 5414 (1989).
[6] D. Ruelle, Ann. Inst. Poincaré *42*, 109 (1985).
[7] W. G. Hoover and B. Moran, Phys. Rev. A, in press.
[8] B. Moran, W. G. Hoover, and S. Bestiale, J. Stat. Phys. *48*, 709 (1987).
[9] W. G. Hoover, B. Moran, C. G. Hoover, and W. J. Evans, Phys. Lett. A *133*, 114 (1988).
[10] S. Nosé, Mol. Phys. *52*, 255 (1984).
[11] S. Nosé, J. Chem. Phys. *81*, 511 (1984).
[12] W. G. Hoover, Phys. Rev. A *31*, 1695 (1985).
[13] D. J. Evans and B. L. Holian, J. Chem. Phys. *83*, 4069 (1985).
[14] H. A. Posch and W. G. Hoover, Phys. Rev. A *38*, 473 (1988).
[15] D. J. Evans, in Ref. [1], page 221.
[16] D. J. Evans and G. P. Morriss, Comput. Phys. Rep. *1*, 297 (1984).
[17] D. J. Evans and G. P. Morriss, Phys. Rev. Lett. *56*, 2172 (1986).
[18] D. J. Evans, W. G. Hoover, B. H. Failor, B. Moran, and A. J. C. Ladd, Phys. Rev. A *28*, 1016 (1983).
[19] D. J. Evans, Phys. Rev. A *34*, 1449 (1986).
[20] V. I. Oseledec, Trans. Moscow Math. Soc. *19*, 197 (1968).
[21] I. Goldhirsch, P.-L. Sulem, and S. A. Orszag, Physica D *27*, 311 (1987).
[22] G. Benettin, L. Galgani, A. Giorgilli, and J. M. Strelcyn, C. R. Acad. Sci., Ser. A *286*, 431 (1978); Meccanica *15*, 9 (1980).
[23] I. Shimada and T. Nagashima, Prog. Theor. Phys. *61*, 1605 (1979).
[24] A. Wolf, J. B. Swift, H. L. Swinney, and J. A. Vastano, Physica D *16*, 285 (1985).
[25] W. G. Hoover and H. A. Posch, Phys. Lett. A *113*, 82 (1985).
[26] W. G. Hoover and H. A. Posch, Phys. Lett. A *123*, 227 (1987).
[27] W. G. Hoover, C. G. Hoover, and H. A. Posch, Phys. Rev. A, in print (1990).
[28] H. A. Posch and W. G. Hoover, Phys. Rev. A *39*, 2175 (1989).
[29] B. L. Holian and D. J. Evans, J. Chem. Phys. *78*, 5147 (1983).
[30] B. L. Holian, Phys. Rev. Lett. *60*, 1355 (1988).
[31] R. Livi, M. Pettini, S. Ruffo, and A. Vulpiani, J. Stat. Phys. *48*, 539 (1987).
[32] W. G. Hoover, H. A. Posch, B. L. Holian, M. L. Gillan, M. Marechal, and C. Massobrio, Mol. Simulation *1*, 79 (1987).
[33] J. Kaplan and J. Yorke, in: Functional Differential Equations and the Approximation of Fixed Points, Vol. 730 of Lecture Notes in Mathematics, eds. H. O. Peitgen and H. O. Walther, Springer-Verlag, Berlin 1980.
[34] J. D. Farmer, E. Ott, and J. A. Yorke, Physica D, *7*, 153 (1983).
[35] T. C. Halsy, M. H. Jensen, L. P. Kadanoff, I. Procaccia, and B. I. Shraiman, Phys. Rev. A *33*, 1141 (1986).
[36] G. Paladin and A. Vulpiani, Phys. Rep. *156*, 147 (1987).
[37] P. Grassberger and I. Procaccia, Physica D *13*, 34 (1984).
[38] A. Chhabra and R. V. Jensen, Phys. Rev. Lett. *62*, 1327 (1989).
[39] G. P. Morriss, Phys. Lett. A *122*, 236 (1987).
[40] G. P. Morriss, Phys. Rev. A *37*, 2118 (1988).
[41] G. P. Morriss, Phys. Lett. A *134*, 307 (1989).
[42] G. P. Morriss, Phys. Rev. A *39*, 4811 (1989).

[43] B. L. Holian, W. G. Hoover, and H. A. Posch, Phys. Rev. Lett. *59*, 10 (1987).
[44] J. Loschmidt, Sitzungsber. Akad. Wiss. Wien, Math. Naturwiss. Kl. Abt. 2, *73*, 128 (1876).
[45] L. Boltzmann, Sitzungsber. Akad. Wiss. Wien, Math. Naturwiss. Kl. Abt. 2, *75*, 67 (1877).

Presented at the Joint Discussion Meeting of the Deutsche Bunsen-Gesellschaft für Physikalische Chemie, Associazione Italiana di Chimica Fisica, Faraday Division of the Royal Society of Chemistry, Société Française de Chimie, Division de Chimie Physique, "Transport Processes in Fluids and in Mobile Phases" Aachen, September 25th to 27th, 1989

E 7240